

# Metal corroles as electrocatalysts for oxygen reduction†

James P. Collman,\* Marina Kaplun and Richard A. Decréau

Received 13th September 2005, Accepted 14th October 2005

First published as an Advance Article on the web 2nd November 2005

DOI: 10.1039/b512982f

The rotating ring disk electrode method has been used to study O<sub>2</sub> electroreduction with metal corroles. Catalysis begins at potentials that are 0.5–0.7 V more positive than the expected potential of the M<sup>III/II</sup> couple based on studies in non-aqueous solutions. The path of O<sub>2</sub> reduction depends on the nature of the metal ion. Cobalt corroles promote O<sub>2</sub> reduction to H<sub>2</sub>O<sub>2</sub>. Iron corroles catalyse O<sub>2</sub> reduction *via* parallel two- and four-electron pathways, with a predominate four-electron reaction. The rate constants for the individual O<sub>2</sub> reduction paths are given at pH 7. Mechanisms are proposed on the basis of pH dependence, inhibition studies, and Tafel slopes. An imidazole-tailed iron corrole catalyses H<sub>2</sub>O<sub>2</sub> disproportionation analogous to catalase.

## Introduction

Metal macrocycles are of interest for electrocatalysis of O<sub>2</sub> reduction because they mimic the active sites of enzymes (*e.g.*, quinol and cytochrome *c* oxidases),<sup>1</sup> and might also be used as electrode materials in technological devices (fuel cells, metal–air batteries, oxygen sensors, *etc.*).<sup>2</sup> Porphyrins and phthalocyanines have been widely studied in a continuing search for catalysts that might promote direct 4e<sup>−</sup> O<sub>2</sub> reduction.<sup>3–6</sup> Herein, we report catalysis of O<sub>2</sub> reduction using several metal complexes of a different lesser studied macrocycle–corrole. Corroles are closely related to porphyrins except they lack one *meso*-carbon and are trianionic ligands stabilizing higher metal oxidation states than porphyrins. Several efficient syntheses had been described lately that made corroles accessible,<sup>7</sup> and have led to studies of their metallo-derivatives as catalysts for oxidation reactions<sup>8</sup> and electroreduction of CO<sub>2</sub>.<sup>9</sup> Recently, a series of Co corroles have been reported as effective catalysts for O<sub>2</sub> reduction<sup>10</sup> that promote parallel 2e<sup>−</sup> and 4e<sup>−</sup> pathways similar to related cofacial Co diporphyrins and porphyrins which can form dimers when adsorbed on an electrode surface.<sup>3,4,6</sup> Our interest has been to identify and compare pathways of O<sub>2</sub> reduction with monomeric corroles that differ in the nature of the central metal ion (M = 3H, Mn, Fe, Co). A highly electron withdrawing corrole with three bulky *meso*-substituents was thought necessary in order to have catalysts that do not form dimers and to raise the potential of the M<sup>III/II</sup> transition,<sup>9</sup> since the potentials where metal complexes catalyse O<sub>2</sub> reduction are usually close to that of the M<sup>III/II</sup> transition of the catalyst, and the M<sup>III/II</sup> potential in corroles is more negative than in the corresponding porphyrins.<sup>11</sup> Therefore we synthesized metal complexes of tris(pentafluorophenyl)corrole 2–4, and of bis(pentafluorophenyl)corrole 5–6 bearing an imidazole axial ligand, which is covalently attached to the corrole macrocycle<sup>7a</sup> (Fig. 1).

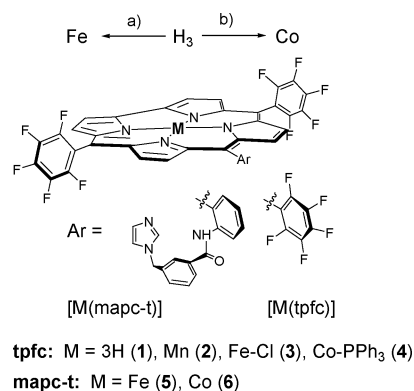


**Fig. 1** Syntheses of compounds 5 and 6, and structure of the studied complexes. *Reagents and conditions:* (a) (i) FeBr<sub>2</sub>, THF–CH<sub>3</sub>OH, AcONa, RT, N<sub>2</sub>; (ii) O<sub>2</sub>; (iii) HCl, CH<sub>2</sub>Cl<sub>2</sub>, 52%; (b) Co(AcO)<sub>2</sub>·4H<sub>2</sub>O, C<sub>2</sub>H<sub>5</sub>OH, AcONa, RT, 2 h, N<sub>2</sub>, 79%. The preparation of compounds 1–4 is described in ref. 12.

## Experimental

### Preparation of the catalysts

5,10,15-Tris(pentafluorophenyl)corrole [H<sub>3</sub>(tpfc)] (1), 5,10,15-tris(pentafluorophenyl)corrole manganese(III) [Mn(tpfc)] (2), 5,10,15-tris(pentafluorophenyl)corrole iron(IV) chloride [Fe(tpfc)Cl] (3), and 5,10,15-tris(pentafluorophenyl)corrole cobalt(III) triphenyl phosphine [Co(tpfc)PPh<sub>3</sub>] (4) were synthesized according to literature procedures.<sup>12</sup>

**5,15-Bis(pentafluorophenyl)-10-(2-3-(1-imidazolylmethyl)-benzamidophenyl)-corrole iron(III) [Fe(mapc-t)] (5).** A solution of free base tailed corrole, H<sub>3</sub>(mapc-t), (50 mg, 53.2 μmol) was stirred with FeBr<sub>2</sub> (36 mg, 165.6 μmol) in a THF/CH<sub>3</sub>OH mixture (4 : 1 vol.) in the presence of sodium acetate (44.0 mg, 532 μmol) at room temperature for 16 h under inert atmosphere. CH<sub>2</sub>Cl<sub>2</sub> was added (100 mL), air was bubbled through the solution for 1 h, and the solution was washed with 7% HCl (2 × 50 mL). After evaporation of the solvent, the residue was subjected to chromatography (SiO<sub>2</sub>, elution hexane/Et<sub>2</sub>O 2 : 1 vol.). 5 crushed out after an excess of hexanes was added to a solution of 5 in EtOH/acetone (1 : 2 vol.). 5 was obtained in 52% yield (17 mg,

Department of Chemistry, Stanford University, Stanford, CA 94305, USA. E-mail: jpc@stanford.edu; Fax: +1 650 7250259; Tel: +1 650 7250283

† Electronic supplementary information (ESI) available: Analysis of electrochemical data, and characterization data for compounds 5 and 6. See DOI: 10.1039/b512982f

purple; pink solution in Et<sub>2</sub>O). <sup>1</sup>H-NMR (400 MHz, CDCl<sub>3</sub>) δ<sub>H</sub>(ppm): 128.26 (2H), 83.28 (2H), 12.53 (2H), 10.02 (2H), 7.69 (2H), 6.96 (2H), 6.47 (2H), 5.12 (2H), -0.08 (1H), -60.22 (2H), -63.42 (2H). <sup>19</sup>F-NMR (400 MHz, C<sub>6</sub>D<sub>6</sub>) δ<sub>F</sub>(ppm): -93.2 (brs, 2F), -110.8 (brs, 2F), -150.78 (s, 2F), -156.05 (s, 2F), -157.67 (s, 2F). UV-Vis. (CH<sub>2</sub>Cl<sub>2</sub>) λ (Abs.) 10<sup>-3</sup> × ε (M<sup>-1</sup> cm<sup>-1</sup>): 328 (10.7), 360 (11.4), 410 (19.3), 552 (5.5), 626 (1.4 sh), 754 (1.6) nm. MS (ESI<sup>+</sup>, *m/z*) = 958.3 [M]<sup>+</sup>, HR-MS (ESI<sup>+</sup>, *m/z*) = 958.1078 (Calcd for C<sub>48</sub>H<sub>22</sub>F<sub>10</sub>FeN<sub>7</sub>O). Anal. Calcd for C<sub>48</sub>H<sub>22</sub>F<sub>10</sub>FeN<sub>7</sub>O·H<sub>2</sub>O·3EtOH: C, 58.18; H, 3.80; N, 8.79; Cl, 0.00; Found: C, 58.56; H, 3.41; N, 8.23; Cl, 0.40. TLC (silica, Et<sub>2</sub>O 100% vol.) R<sub>f</sub> 0.72.

**5,15-Bis(pentafluorophenyl)-10-(2-3-(1-imidazolylmethyl)-benzamidophenyl)-corrole cobalt(III) [Co(mapc-t)] (6).** Corrole **6** was prepared from the adaptation of a reported method<sup>12c</sup> by dissolving H<sub>3</sub>(mapc-t) (22.6 mg, 25 μmol), Co(OAc)<sub>2</sub>·4H<sub>2</sub>O (30 mg, 120 μmol) and NaOAc (30 mg, 366 μmol) in ethanol (10 mL) and stirring the resulting solution for 2 h at 25 °C. After evaporation of the solvent, the residue was subjected to chromatography (SiO<sub>2</sub>, 17 × 2 cm, loading CH<sub>2</sub>Cl<sub>2</sub>, eluent CH<sub>2</sub>Cl<sub>2</sub>). **6** was obtained in 78.8% yield (19 mg, dark brown; brown solution in CH<sub>2</sub>Cl<sub>2</sub>). Limited amount of dimer was obtained. <sup>1</sup>H-NMR (400 MHz, CDCl<sub>3</sub>) δ<sub>H</sub>(ppm): 9.02 (d, 2H, *J* = 4.4 Hz), 8.95 (d, 1H, *J* = 6.8 Hz), 8.37 (d, 2H, *J* = 4.8 Hz), 8.18 (d, 2H, *J* = 4.8 Hz), 8.12 (d, 2H, *J* = 4.4 Hz), 7.95 (d, 1H, *J* = 6.0 Hz), 7.88 (s, 1H), 7.86 (s, 1H), 7.77 (t, 1H, *J* = 7.2 Hz), 7.40 (t, 1H, *J* = 6.0 Hz), 7.19 (t, 1H, *J* = 6.0 Hz), 6.77 (d, 1H, *J* = 5.6 Hz), 5.02 (s, 1H), 4.06 (s, 1H), 3.89 (s, 2H), 3.28 (s, 1H), 2.58 (s, 1H). <sup>19</sup>F-NMR (400 MHz, CDCl<sub>3</sub>) δ<sub>F</sub>(ppm): -137.52 (dd, *J* = 25.2 Hz, *J* = 7.6 Hz, 2F), -139.45 (dd, *J* = 26.0 Hz, *J* = 7.6 Hz, 2F), -153.62 (t, *J* = 19.6 Hz, 2F), -161.35 (dt, *J* = 25.2 Hz, 2F), -162.26 (dt, *J* = 26.0 Hz, 2F). <sup>13</sup>C-NMR (75 MHz, CDCl<sub>3</sub>) δ<sub>C</sub>(ppm): 163.25, 150.14, 147.26, 145.97, 144.89, 143.00, 138.62, 136.81, 135.57, 135.47, 135.23, 132.64, 130.98, 130.53, 129.66, 129.62, 129.14, 128.57, 128.31, 127.91, 127.57, 125.83, 123.75, 121.98, 120.74, 120.41, 119.58, 118.71, 116.95, 106.80, 50.17, 29.93. UV-Vis. (CH<sub>2</sub>Cl<sub>2</sub>) λ (Abs.) 10<sup>-3</sup> × ε (M<sup>-1</sup> cm<sup>-1</sup>): 380 (47.7), 412 (26.2), 546 (7.4), 586 (4.3), 604 (4.2) nm. MS (ESI<sup>+</sup>, *m/z*) = 961.5 [M]<sup>+</sup>, HR-MS (ESI<sup>+</sup>, *m/z*) = 961.1091, MS (ESI<sup>-</sup>, *m/z*) = 960.5 [M - H]<sup>-</sup> (Calcd for C<sub>48</sub>H<sub>22</sub>CoF<sub>10</sub>N<sub>7</sub>O). TLC (silica, CH<sub>2</sub>Cl<sub>2</sub> 100% vol.) R<sub>f</sub> 0.53 (silica, hexane/ethyl acetate 1 : 1 vol.) R<sub>f</sub> 0.70.

## Materials

KNO<sub>3</sub> (≥ 99%, Acros) was recrystallized. NaCN (≥ 95%, Baker & Adamson) was used as supplied. WARNING: Cyanide is highly toxic, the experiments must be performed in a properly ventilated area. All discarded electrolytes were neutralized with bleach before disposal. The buffers employed were (0.1 M): KC<sub>8</sub>H<sub>5</sub>O<sub>4</sub>, pH = 4; KH<sub>2</sub>PO<sub>4</sub>, pH = 4.4; Na<sub>2</sub>HPO<sub>4</sub>/KH<sub>2</sub>PO<sub>4</sub>, pH = 5.1, 6.2, 7, 8; Na<sub>2</sub>CO<sub>3</sub>/NaHCO<sub>3</sub>, pH = 9; Na<sub>3</sub>PO<sub>4</sub>/NaHCO<sub>3</sub>, pH = 10, 11.

## Procedures and instrumentation

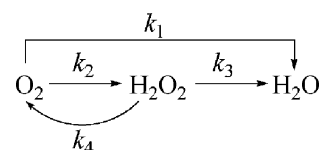
Experiments were carried out in a one compartment home-made glass cell (100 mL) with a tightly fitting lid using an edge plane graphite (EPG) rotating disk working electrode (Pine Instruments, 0.195 cm<sup>2</sup>) or a ring-disk electrode with a removable EPG disk

and Pt ring (Pine Instruments, *N*<sub>0</sub> = 22.5%, *r*<sub>10</sub> = 2.5 mm, *r*<sub>20</sub> = 3.75 mm, and *r*<sub>30</sub> = 4.25 mm). The collection efficiency of the Pt ring towards H<sub>2</sub>O<sub>2</sub> was determined as a function of the rotation speed<sup>13</sup> by carrying out the O<sub>2</sub> reduction at a bare EPG disk of the EPG-disk/Pt-ring rotating electrode. A BAS CV-50 W potentiostat (Bioanalytical Systems) and a Pine AFCBP1 bipotentiostat (Pine Instruments) with an ASR speed controller (Pine Instruments) were used for rotating disk and ring-disk experiments, respectively. The auxiliary electrode was a Pt mesh and the reference electrode was a low flow rate saturated calomel electrode. All potentials are given with respect to the normal hydrogen electrode (*E*<sub>SCE</sub> = 0.243 V vs. NHE).

The Pt ring was cleaned with 0.05 micron γ-alumina paste for 1 min followed by sonication in methanol. The EPG disk was cleaned with a 600 grit SiC paper and sonicated for 1 min in methanol immediately prior to depositing a catalytic film. The catalysts were deposited on the electrode surface by syringing a 0.6–2.0 μL aliquot of a fresh 0.25–0.5 mM solution in a dimethoxyethane/water mixture (5.6 : 1 vol.) or acetone on a vertically positioned rotating electrode (300 rpm). The stability of the catalysts was verified in every experiment by measuring the voltammetric response at 200 rpm before and after the set of catalytic waves at different rotations was collected. The limiting current value varied by only 2–4%. The presented data are representative of at least 10 separate measurements. Measurements were conducted at ambient temperature, 22 ± 2 °C, in N<sub>2</sub> deaerated solutions when necessary.

## Kinetic analysis

The following simplified general scheme of O<sub>2</sub> reduction was used to analyse the data:



O<sub>2</sub> is cathodically reduced either to H<sub>2</sub>O (with the constant *k*<sub>1</sub>) or to H<sub>2</sub>O<sub>2</sub> (*k*<sub>2</sub>). The resulting H<sub>2</sub>O<sub>2</sub> can be further reduced to H<sub>2</sub>O (*k*<sub>3</sub>), catalytically decomposed on the electrode surface (*k*<sub>4</sub>), or removed into the bulk of the solution.

For such a scheme, the expressions for distinguishing between various reaction paths from the disk (*I*<sub>d</sub>) and ring (*I*<sub>r</sub>) currents were developed by Bagotskii:<sup>14</sup>

$$\frac{NI_d}{I_r} = 1 + \frac{2k_1}{k_2} + \frac{(k_3 + k_4)(1 + 2k_1/k_2) + k_3}{Z_{\text{H}_2\text{O}_2}} \omega^{-1/2} \quad (1)$$

$$\frac{N(I_1 - I_d)}{I_r} = 1 + \frac{2Z_{\text{O}_2}}{Z_{\text{H}_2\text{O}_2}} \frac{k_3 + k_4}{k_2} + \frac{2Z_{\text{O}_2}}{k_2} \omega^{1/2} \quad (2)$$

where *I*<sub>d</sub> and *I*<sub>r</sub> (*A*) are the disk and the ring currents, *I*<sub>1</sub> (*A*) is the limiting diffusion current, *N* is the collection efficiency of the ring electrode, *Z*<sub>i</sub> = 0.62*D*<sub>i</sub><sup>2/3</sup>*v*<sup>-1/6</sup>, *D* (cm<sup>2</sup> s<sup>-1</sup>) is a diffusion coefficient, *v* (cm<sup>2</sup> s<sup>-1</sup>) is the kinematic viscosity of the solution, ω (rad s<sup>-1</sup>) is the speed of electrode rotation, *k*<sub>i</sub> (cm s<sup>-1</sup>) are the first-order heterogeneous rate constants for individual paths of O<sub>2</sub> reduction. The values of the parameters are: *D* = 1.71 × 10<sup>-5</sup> (H<sub>2</sub>O<sub>2</sub>) and 2.1 × 10<sup>-5</sup> cm<sup>2</sup> s<sup>-1</sup> (O<sub>2</sub>), *v* = 0.01 cm<sup>2</sup> s<sup>-1</sup>, [O<sub>2</sub>] = 0.24 mM, *I*<sub>1</sub> = 84 μA for a 4e<sup>-</sup> process.

## Results and discussion

### Redox properties of the catalysts

The redox properties of the catalysts were studied by cyclic voltammetry. The iron corroles adsorbed on edge-plane graphite (EPG) disk electrode show two redox couples at 0.66 V and  $-0.50$  V vs. NHE for Fe(tpfc)Cl and 0.71 V and  $-0.63$  V for Fe(mapc-t) (Fig. 2). Comparison with spectroelectrochemical data in acetonitrile<sup>9</sup> suggests that these redox processes should be Fe<sup>IV/III</sup> and Fe<sup>III/II</sup> transitions. To verify the proposed assignments, we examined the effects of pH and of the addition of ligands to the solution. The potential of the higher couple in Fe(tpfc)Cl shifts by  $-60$  mV pH<sup>-1</sup> (Fig. 3), in accord with the Fe<sup>IV/III</sup> assignment. The lower transition does not depend on pH and is shifted to more negative potentials in the presence of imidazole, as expected for the Fe<sup>III/II</sup> process. Surprisingly, this couple is not sensitive to CN<sup>-</sup>, and is not linked to O<sub>2</sub> reduction, as the redox peaks persist in air-saturated solution (Fig. 2). Thus, it seems likely that this redox process is ligand-centered (*vide infra*). The process can not be ascribed to Fe<sup>III/I</sup> transition because the electrode potential of Fe<sup>II/I</sup> in acetonitrile is  $-1.60$  V vs. SCE.<sup>9</sup>

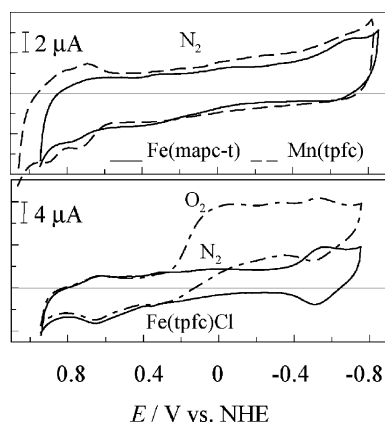


**Fig. 2** Cyclic voltammograms for the Fe and Mn corroles in N<sub>2</sub> deaerated and air-saturated 0.1 M KNO<sub>3</sub>, pH 7, scan rate: 0.05 V s<sup>-1</sup>, coverage: 2.56 nmol cm<sup>-2</sup>.

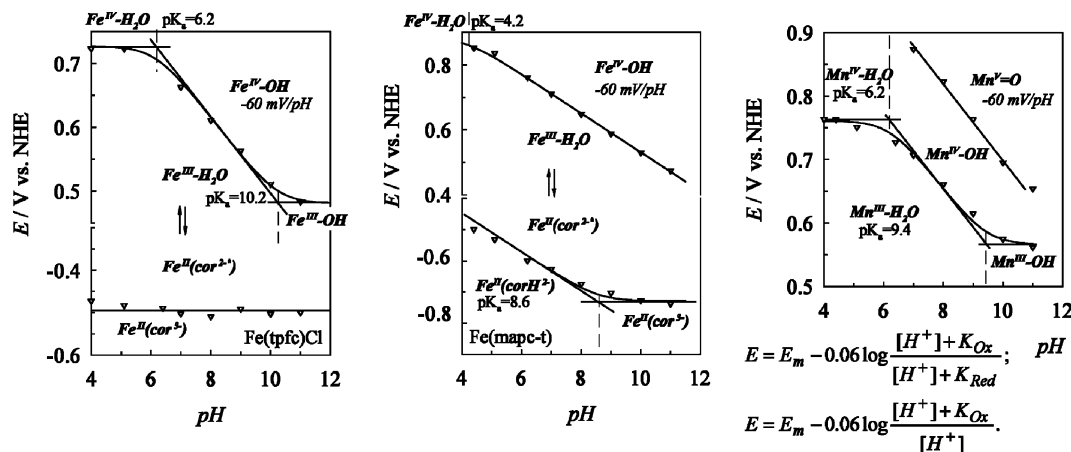


**Fig. 3** The redox potentials of Fe(tpfc)Cl, Fe(mapc-t), and Mn(tpfc) as a function of pH. pK<sub>a</sub> values are obtained from the curve-fit of the appropriate Nernst–Clark equation (ref. 15) to the experimental data. The potential of the invoked intramolecular electron transfer Fe<sup>III</sup>(cor<sup>2+</sup>)/Fe<sup>II</sup>(cor<sup>2+</sup>) is not presently clear (see text for details).

Mn(tpfc) shows redox couples at 0.88 V and 0.73 V at pH 7. Both peaks shift by  $-60$  mV pH<sup>-1</sup> and are sensitive to the presence of imidazole. Therefore, the redox processes are proposed to be Mn<sup>V/IV</sup> and Mn<sup>IV/III</sup> transitions (Fig. 3). Cobalt corroles do not exhibit well-defined redox peaks when adsorbed on EPG. This behavior has previously been observed for Co complexes, and was suggested to arise from different coordination preferences of Co<sup>III</sup> and Co<sup>II</sup>.<sup>3d</sup> In our discussion, we have used the Co<sup>III/II</sup> reduction potentials in acetonitrile (*ca.*  $-0.16$  V vs. NHE).<sup>9</sup>

### Electrocatalysis of O<sub>2</sub> reduction

Electrocatalysis of O<sub>2</sub> reduction was studied by rotating ring-disk electrode voltammetry<sup>16</sup> in air-saturated aqueous solutions. The currents for O<sub>2</sub> electroreduction using selected metal corroles adsorbed on the EPG disk electrode, as well as the corresponding limiting currents of H<sub>2</sub>O<sub>2</sub> oxidation on the Pt ring electrode at pH 7 are shown in Fig. 4A. The presence of Co and Fe corroles on the disk electrode causes a positive shift in the half-wave potential of O<sub>2</sub> reduction by 0.4–0.2 V, while the activity of H<sub>3</sub>(tpfc) (not presented) and Mn(tpfc) is comparable to that of bare EPG.

Free base, Mn, and Co corroles<sup>17</sup> catalyse only 2e<sup>-</sup> reduction to H<sub>2</sub>O<sub>2</sub> as evidenced by the correspondence of the ring and disk currents, and by the number of electrons found from the slope of the Koutecky–Levich plots (1/I<sub>d</sub> vs. ω<sup>-1/2</sup>).<sup>16</sup> Additional support comes from a separate study of the catalysts in 0.25 mM H<sub>2</sub>O<sub>2</sub> solution which showed no significant H<sub>2</sub>O<sub>2</sub> reduction activity (Fig. 4B, curves 3–5).

With Fe corroles as precatalysts, the larger catalytic currents and the lower ring currents (Fig. 4A) show that much less H<sub>2</sub>O<sub>2</sub> is produced and are indicative of involvement of a 4e<sup>-</sup> pathway. For Fe(tpfc)Cl, two waves involving O<sub>2</sub> reduction are observed in the disk current with corresponding waves of H<sub>2</sub>O<sub>2</sub> oxidation in the ring current. The number of electrons on the plateaus of the waves is 3.6 and 4, respectively, indicating that the two waves are not a result of (2 + 2)e<sup>-</sup> reduction but originate from catalysis by two active forms of the catalyst. Further analysis of the data using eqn (1) and (2) (by plotting the data at desired potential

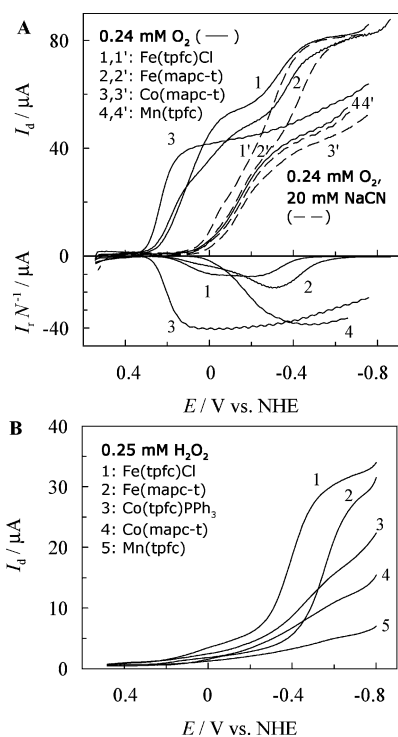


**Fig. 4** (A) Rotating ring-disk electrode data for the reduction of  $O_2$  in the absence (solid lines) and presence of 20 mM NaCN (dashed lines) at: (1,1') Fe(tpfc)Cl; (2,2') Fe(mapc-t); (3,3') Co(mapc-t); (4,4') Mn(tpfc) in 0.1 M  $KNO_3$  at pH 7,  $E_{ring} = 0.5$  V vs. SCE, scan rate:  $0.02$  V  $s^{-1}$ , rotation speed: 200 rpm, coverage:  $1.5$  nmol  $cm^{-2}$ . (B) Rotating disk electrode data for the reduction of  $0.25$  mM  $H_2O_2$  at: (1) Fe(tpfc)Cl; (2) Fe(mapc-t); (3) Co(tpfc)PPh<sub>3</sub>; (4) Co(mapc-t); (5) Mn(tpfc) in 0.1 M  $KNO_3$  at pH 7, scan rate:  $0.02$  V  $s^{-1}$ , rotation speed: 200 rpm, coverage:  $1.5$  nmol  $cm^{-2}$ .

as  $NI_d/I_r$  vs.  $\omega^{-1/2}$  and  $N(I_1 - I_d)/I_r$  vs.  $\omega^{1/2}$ ) shows that for all potentials where  $H_2O_2$  is detected,  $O_2$  is reduced by parallel  $2e^-$  and  $4e^-$  pathways. The  $k_1/k_2$  ratio varies from 2 to 12 (Fig. 5), and thus  $O_2$  is predominantly reduced to water.

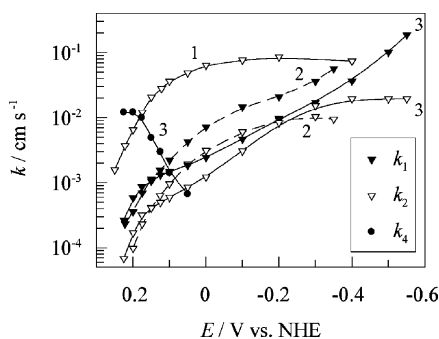


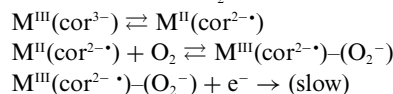
**Fig. 5** Potential dependence of the heterogeneous rate constants for the  $2e^-$  ( $k_2$ ) and  $4e^-$  ( $k_1$ ) reduction of  $O_2$  and for catalytic dismutation of  $H_2O_2$  ( $k_4$ ) at: (1) Co(mapc-t); (2) Fe(tpfc)Cl; (3) Fe(mapc-t).

Similar reduction paths are drawn for catalysis on Fe(mapc-t) at negative potentials. An additional wave above 0 V is explained as dismutation of intermediate  $H_2O_2$  based on the treatment of the data giving  $(k_3 + k_4) \neq 0$  and on the fact that the catalyst is not active toward  $H_2O_2$  reduction ( $k_3 = 0$ ) in this potential range (Fig. 4B). The calculated rate constant ( $k_4$ , Fig. 5) depends

on potential, which indicates that the number of the active sites (supposedly,  $Fe^{III}-O_2H$  intermediate or/and  $Fe^{III}$  form of corrole, *vide infra*) decreases with reducing potential. The value of  $4.0 \times 10^3$   $M^{-1} s^{-1}$  estimated at 0.2 V is *ca.* 4 orders of magnitude less than that for dismutation by catalase<sup>18a</sup> but among the largest reported for synthetic  $Fe^{III}$  complexes (*ca.*  $1.5 \times 10^3$   $M^{-1} s^{-1}$ ).<sup>5e,18b</sup>

Catalysis of  $O_2$  reduction by Co and Fe corroles begins at potentials ( $E \cong 0.3$  V vs. NHE) that are 0.5–0.7 V more positive than the expected potential of the  $M^{III/II}$  couple based on studies in non-aqueous solutions, as recently observed in Kadish *et al.*<sup>10</sup> where the onset of catalytic waves correlates with the  $Co^{IV/III}$  potential of the catalysts. This is unusual considering that  $M^{III}$  is not expected to bind  $O_2$  and hence should not be catalytically active. To probe the nature of the active sites (metal ion vs. ligand), we performed inhibition experiments in air-saturated 20 mM NaCN solutions. The results indicate that  $O_2$  activation occurs at the metal center, because the reduction waves in the potential range of the  $M^{III}$  form of the catalysts are strongly suppressed in the presence of  $CN^-$  (Fig. 4A, dashed lines). Thus, it seems reasonable to propose the presence of the  $M^{II}$  form, which may arise from an internal corrole-to-metal(III) electron transfer,  $M^{III}(cor^{3-}) \rightleftharpoons M^{II}(cor^{2-\cdot})$ ,<sup>19</sup> that is inhibited by  $CN^-$  due to stabilization of the  $M^{III}$  oxidation state. The waves at higher reducing potentials are not sensitive to  $CN^-$ , suggesting a  $M^{II}(cor^{2-\cdot}) + e^- \rightleftharpoons M^{II}(cor^{3-})$  redox transition in the catalysts based on a low affinity of  $CN^-$  for  $M^{II}$ .<sup>20</sup>

Two plausible mechanisms of  $O_2$  reduction are suggested to account for the observed results. One possibility is that the  $M^{II}$  form reacts relatively fast with  $O_2$  if we assume that the onset of  $O_2$  reduction correlates with the potential of the proposed electron transfer (the mechanism typical of  $O_2$  catalysis with iron porphyrins), and thus  $M^{II}(cor^{2-\cdot})$  form becomes favored at  $E \leq 0.3$  V.<sup>21</sup> Alternatively, the  $M^{II}(cor^{2-\cdot})$  form might arise directly from the  $M^{IV/III}$  transition, suggesting a slow formation of an  $O_2$  adduct which is reduced at more negative potentials.<sup>3c</sup> Tafel plots (applied potential vs. the log. of the kinetic current or rate constants) constructed for  $O_2$  reduction on  $H_3$ (tpfc), Mn(tpfc), and Fe(tpfc)Cl, show slopes of  $-120$  mV  $dec^{-1}$ , indicating that the rate of the overall turnover is determined by a first electron transfer to adsorbed  $O_2$ :<sup>4</sup>



Catalysis on Fe(mapc-t) and Co corroles shows Tafel slopes of  $-60$  mV  $dec^{-1}$ , suggesting the slow chemical step (*e.g.*,  $O_2$  binding or further protonation of the adduct).<sup>4</sup>

The pH dependence of  $O_2$  reduction was examined with Co and Fe corroles. On Co corroles, the Tafel slopes are pH dependent and decrease gradually from  $-86$  mV  $dec^{-1}$  to  $-42$  mV  $dec^{-1}$  over the pH range 4–11 (Fig. 6). The pH dependence of potential has a slope of  $-40$  mV  $pH^{-1}$  (Fig. 7A), giving pH dependent order in protons,  $p(H^+) = (\partial E/\partial pH)/(\partial E/\partial \log k)$ . The data indicate a different mechanism in alkaline solutions with the rate determining first electron transfer. On Fe(tpfc)Cl, the mechanism does not change with pH as the Tafel slopes are  $-120$  mV  $dec^{-1}$  at all studied pHs, and the potential shows a weak pH dependence. On Fe(mapc-t), the rate of dismutation goes through a maximum at pH 9 (Fig. 7B). Kinetic parameters of individual paths were not determined because of insufficiently long linear parts of the Tafel

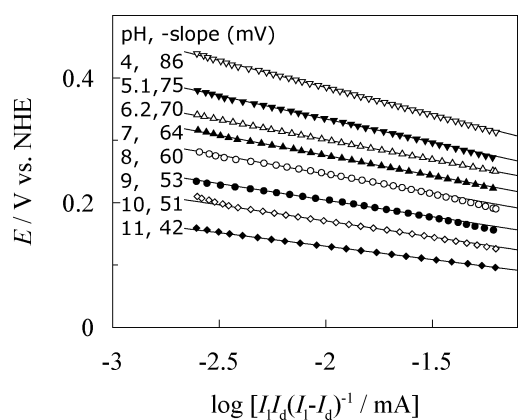


Fig. 6 Tafel plots for the reduction of O<sub>2</sub> at Co(mapc-t) in 0.1 M KNO<sub>3</sub> solutions of different pH.

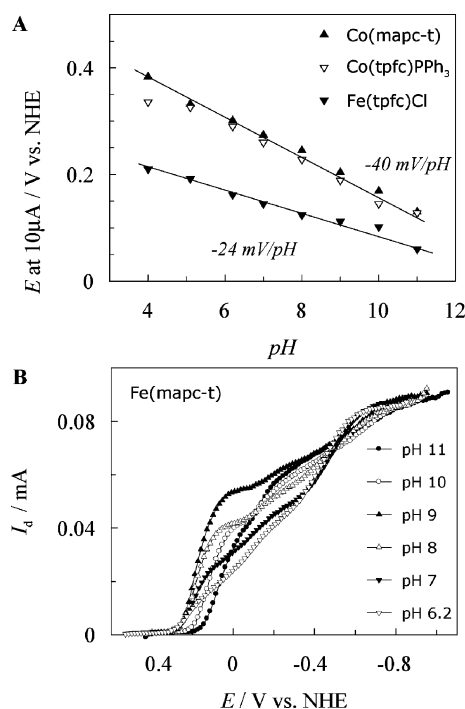


Fig. 7 (A) Plots of potential at constant current (10 μA) vs. pH for the reduction of O<sub>2</sub> on cobalt and iron corroles derived from corresponding Tafel plots. (B) The currents of O<sub>2</sub> electroreduction at Fe(mapc-t) at different pH, scan rate: 0.04 V s<sup>-1</sup>, rotation speed: 200 rpm.

plots. These kinetic data correspond to the first reduction wave. The mechanism at more negative potentials was not analysed due to overlap of the second reduction wave (ascribed to catalysis by M<sup>II</sup>(cor<sup>3-</sup>) form) with residual catalysis by the first active form of the catalysts, M<sup>II</sup>(cor<sup>2-</sup>), and with possible contribution from catalysis by EPG due to the porous nature of the catalytic layer.

## Conclusions

In summary, we have demonstrated that metal corroles adsorbed on EPG electrode operate at potentials comparable with those observed for catalysis with metal porphyrins and are effective cat-

alysts for O<sub>2</sub> reduction. The activity series is similar to tetraphenylporphyrins and dibenzo-tetraazaannulenes: Co > Fe ≫ Mn, 3H. The behavior of Co, Mn and H<sub>3</sub> corroles parallels findings on related porphyrins, whereas the results from the Fe corroles show remarkable differences. First, the Fe corroles promote O<sub>2</sub> reduction to H<sub>2</sub>O directly, rather than by the (2 + 2)e<sup>-</sup> pathway typical of Fe porphyrins. Second, the activity for H<sub>2</sub>O<sub>2</sub> reduction is less than that for O<sub>2</sub> reduction, whereas for Fe porphyrins the activities are similar. Reduction of H<sub>2</sub>O<sub>2</sub> is observed only at E ≤ -0.3V (k<sub>3</sub>/coverage ≅ 2 × 10<sup>4</sup> M<sup>-1</sup> s<sup>-1</sup> at -0.6 V), which might be explained by inhibition of a supposed intramolecular transition in the catalysts due to H<sub>2</sub>O<sub>2</sub> reacting with Fe<sup>III</sup> through a homolytic process.

## Acknowledgements

Work was supported by NIH (Grant No. 5R01 GM-17880-35) and NSF (Grant No. CHE-0131206). R. A. D. thanks the French Foreign Ministry for a Lavoisier fellowship.

## References and notes

- J. Abramson, S. Riistama, G. Larsson, A. Jasaitis, M. Svensson-Ek, L. Laakkonen, A. Puustinen, S. Iwata and M. Wikström, *Nat. Struct. Biol.*, 2000, **7**, 910; D. Zaslavsky and R. B. Gennis, *Biochim. Biophys. Acta*, 2000, **1458**, 164; S. Ferguson-Miller and G. T. Babcock, *Chem. Rev.*, 1996, **96**, 2889.
- A. Bettelheim, L. Soifer and E. Korin, *J. Power Sources*, 2004, **130**, 158; Y. Kiros, O. Lindström and T. Kaimakis, *J. Power Sources*, 1993, **45**, 219; B. Shentu, K. Oyaizu and H. Nishide, *J. Mater. Chem.*, 2004, **14**, 3308.
- (a) J. P. Collman, R. Boulatov, C. J. Sunderland and L. Fu, *Chem. Rev.*, 2004, **104**, 561; (b) M. R. Tarasevich and K. A. Radyushkina, *Russ. Chem. Rev.*, 1980, **49**, 718; (c) J. H. Zagal, *Coord. Chem. Rev.*, 1992, **119**, 89; (d) E. Song, C. Shi and F. C. Anson, *Langmuir*, 1998, **14**, 4315; (e) C.-L. Ni and F. C. Anson, *Inorg. Chem.*, 1985, **24**, 4754; (f) H. Jahnke, M. Schönborn and G. Zimmermann, *Top. Curr. Chem.*, 1976, **61**, 133.
- F. Van den Brink, W. Visscher and E. Barendrecht, *J. Electroanal. Chem.*, 1983, **157**, 305; J. Zagal, P. Bindra and E. Yeager, *J. Electrochem. Soc.*, 1980, **127**, 1506.
- (a) H. Behret, W. Clauberg and G. Sandstede, *Ber. Bunsenges. Phys. Chem.*, 1979, **83**, 139; (b) H. Behret, W. Clauberg and G. Sandstede, *Z. Phys. Chem.*, 1978, **113**, 97; (c) T. Sawaguchi, T. Matsue, K. Itaya and I. Uchida, *Electrochim. Acta*, 1991, **36**, 703; (d) F. Van den Brink, W. Visscher and E. Barendrecht, *J. Electroanal. Chem.*, 1984, **172**, 301; (e) R. Boulatov, J. P. Collman, I. M. Shiryayeva and C. J. Sunderland, *J. Am. Chem. Soc.*, 2002, **124**, 11923.
- C.-L. Ni, I. Abdalamuhdi, C. K. Chang and F. C. Anson, *J. Phys. Chem.*, 1987, **91**, 1158; J. P. Collman, N. H. Hendricks, K. Kim and C. S. Bencosme, *J. Chem. Soc., Chem. Commun.*, 1987, 1537; F. D'Souza, Y. Y. Hsieh and G. R. Deviprasad, *Chem. Commun.*, 1998, 1027.
- (a) E. Rose, A. Kossanyi, M. Quelquejeu, M. Soleilhavoup, F. Duwavan, N. Bernard and A. Lécas, *J. Am. Chem. Soc.*, 1996, **118**, 1567; (b) Z. Gross, N. Galili and I. Saltsman, *Angew. Chem., Int. Ed.*, 1999, **38**, 1427; (c) R. Paolesse, L. Jaquinod, D. J. Nurco, S. Mini, F. Sagone, T. Boschi and K. M. Smith, *Chem. Commun.*, 1999, 1307; (d) Z. Gross, N. Galili, L. Simkhovich, I. Saltsman, M. Botoshansky, D. Blaser, R. Boese and I. Goldberg, *Org. Lett.*, 1999, **4**, 599; (e) R. Paolesse, S. Nardis, F. Sagone and R. G. Khoury, *J. Org. Chem.*, 2001, **66**, 550; (f) D. T. Gryko and K. Jadach, *J. Org. Chem.*, 2001, **66**, 4267; (g) B. Ramdhanie, C. L. Stern and D. P. Goldberg, *J. Am. Chem. Soc.*, 2001, **123**, 9447; (h) R. Guilard, D. T. Gryko, G. Canard, J. M. Barbe, B. Koszarna, S. Brandes and M. Tasior, *Org. Lett.*, 2002, **4**, 4491; (i) J. Sankar, V. G. Anand, S. Venkatraman, H. Rath and T. K. Chandrasekar, *Org. Lett.*, 2002, **4**, 4233; (j) D. T. Gryko, *Eur. J. Org. Chem.*, 2002, **11**, 1735; (k) R. Paolesse, A. Marini, S. Nardis, A. Froiio, F. Mandoj, D. J. Nurco, L. Prodi, M. Montalti and K. M. Smith,

- J. Porphyrins Phthalocyanines*, 2003, **7**, 25; (l) R. A. Decréau and J. P. Collman, *Tetrahedron Lett.*, 2003, **44**, 3323; (m) G. R. Geier, J. F. B. Chick, J. B. Callinan, C. G. Reid and W. P. Auguscinski, *J. Org. Chem.*, 2004, **69**, 4159; (n) J. P. Collman and R. A. Decréau, *Org. Lett.*, 2005, **7**, 975.
- 8 Z. Gross and H. B. Gray, *Adv. Synth. Catal.*, 2004, **346**, 165.
- 9 J. Grodkowski, P. Neta, E. Fujita, A. Mahammed, L. Simkhovich and Z. Gross, *J. Phys. Chem. A*, 2002, **106**, 4772.
- 10 K. M. Kadish, L. Frémond, Z. Ou, J. Shao, C. Shi, F. C. Anson, F. Burdet, C. P. Gros, J.-M. Barbe and R. Guillard, *J. Am. Chem. Soc.*, 2005, **127**, 5625.
- 11 V. A. Adamian, F. D'Souza, S. Licocchia, M. L. Di Vona, E. Tassoni, R. Paolesse, T. Boschi and K. M. Kadish, *Inorg. Chem.*, 1995, **34**, 532; E. Van Caemelbecke, S. Will, M. Autret, V. A. Adamian, J. Lex, J.-P. Gisselbrecht, M. Gross, E. Vogel and K. M. Kadish, *Inorg. Chem.*, 1996, **35**, 184.
- 12 (a) Z. Gross, G. Golubkov and L. Simkhovich, *Angew. Chem., Int. Ed.*, 2000, **39**, 4045; (b) L. Simkhovich, A. Mahammed, I. Goldberg and Z. Gross, *Chem. Eur. J.*, 2001, **7**, 1041; (c) A. Mahammed, I. Giladi, I. Goldberg and Z. Gross, *Chem. Eur. J.*, 2001, **7**, 4259; (d) J. P. Collman and R. A. Decréau, *Tetrahedron Lett.*, 2003, **44**, 1207.
- 13 T. Geiger and F. C. Anson, *Anal. Chem.*, 1980, **52**, 2448.
- 14 V. S. Bagotskii, V. Yu. Filinovskii and N. A. Shumilova, *Russ. J. Electrochem.*, 1968, **4**, 1129; K.-L. Hsueh and D.-T. Chin, *J. Electroanal. Chem.*, 1983, **153**, 79.
- 15 W. M. Clark, *Oxidation-Reduction Potentials of Organic Systems*, Baltimore, Williams & Wilkins, 1960.
- 16 A. J. Bard and L. R. Faulkner, *Electrochemical Methods*, Wiley, New York, 2001.
- 17 The behavior of Co(tpfc)PPh<sub>3</sub> and Co(mapc-t) is the same; Co(tpfc) without an axial base is unstable and could not be isolated, as previously reported in ref. 12c.
- 18 (a) G. R. Schonbaum and B. Chance, In *The Enzymes*, 3rd edn., ed. P. D. Boyer, Academic Press, New York, 1976, **13**, 363; (b) J. Paschke, M. Kirsch, H.-G. Korth, H. de Groot and R. Sustmann, *J. Am. Chem. Soc.*, 2001, **123**, 11099.
- 19 (a) A similar electron transfer was reported for Fe catecholate (ref. 19a), Cu corroles (ref. 19b,c) and Rh porphyrins (ref. 19d): D. D. Cox and L. Que, Jr., *J. Am. Chem. Soc.*, 1988, **110**, 8085; (b) C. Brückner, R. P. Briñas and J. A. Krause Bauer, *Inorg. Chem.*, 2003, **42**, 4495; (c) R. Guillard, C. P. Gros, J.-M. Barbe, E. Espinosa, F. Jérôme, A. Tabard, J.-M. Latour, J. Shao, Z. Ou and K. M. Kadish, *Inorg. Chem.*, 2004, **43**, 7441; (d) J. P. Collman and R. Boulatov, *J. Am. Chem. Soc.*, 2000, **122**, 11812.
- 20 A possible reason is electronic repulsion of CN<sup>-</sup> due to the negative charge of M<sup>II</sup>(cor<sup>3-</sup>) as suggested in: B. Ramdhanie, J. Telser, A. Caneschi, L. N. Zakharov, A. L. Rheingold and D. P. Goldberg, *J. Am. Chem. Soc.*, 2004, **126**, 2515; N. S. Hush and I. S. Woolsey, *J. Chem. Soc., Dalton Trans.*, 1974, 24.
- 21 The reason for and the potential of the invoked internal electron transfer are not presently clear. A possible explanation is that at reducing potentials the electrode becomes negatively charged and can favour the electronic state of the adsorbed species which is avoided when the potential is maintained at positive values; by analogy with the well-known phenomenon of the reorientation of adsorbed aromatic substances (flat orientation vs. vertical one): B. B. Damaskin, O. A. Petrii and V. B. Batrakov, *Adsorption of Organic Compounds on Electrodes*, New York, Plenum Press, 1971.